Signal Processing: *Image Communication* 28 (2013) 1143–1155

Contents lists available at ScienceDirect

Signal Processing: *Image Communication*

journal homepage: www.elsevier.com/locate/image

Full-reference quality assessment of stereopairs accounting for rivalry

Ming-Jun Chen [a,*], Che-Chun Su [a], Do-Kyoung Kwon [b], Lawrence K. Cormack [c], Alan C. Bovik [a]

[a] *LIVE Laboratory, Department of Electrical and Computer Engineering, University of Texas, Austin, TX 78712, USA*
[b] *Systems and Applications R&D Center, Texas Instrument, Dallas, TX 75243, United States*
[c] *The Center for Perceptual Systems and the Department of Psychology, University of Texas at Austin, Austin, TX 78712, USA*

ARTICLE INFO

Article history:
Received 1 November 2012
Received in revised form
31 March 2013
Accepted 31 May 2013
Available online 21 June 2013

Keywords:
Binocular rivalry
Image quality
Stereoscopic quality assessment
Stereo algorithm

ABSTRACT

We develop a framework for assessing the quality of stereoscopic images that have been afflicted by possibly asymmetric distortions. An intermediate image is generated which when viewed stereoscopically is designed to have a perceived quality close to that of the cyclopean image. We hypothesize that performing stereoscopic QA on the intermediate image yields higher correlations with human subjective judgments. The experimental results confirm the hypothesis and show that the proposed framework significantly outperforms conventional 2D QA metrics when predicting the quality of stereoscopically viewed images that may have been asymmetrically distorted.

1. Introduction

Stereoscopic vision was first systematically studied by Wheatstone [1] in the early 1800s and the production of 3D films can be dated back to 1903 [2]. Since then, numerous 3D films have been produced, culminating in the breakout success of *Avatar* in 2009, which went on to become the highest-grossing film of all time. The success of *Avatar* has since greatly inspired further efforts in 3D film production and improved technologies and methods for 3D content capture and display.

Indeed, the wave of 3D has not been limited to the theater screen. In 2011, mobile phones supporting 3D capture and viewing are now available, the number of released 3D films has tripled compared to the number in 2008 [2], and broadcast 3D content over the Internet is becoming common [3]. With the release of 3D phones and 3D broadcast services, it is reasonable to believe that the amount of 3D content that is delivered by wireless and wireline will follow the trend of consumer video and increase exponentially over the next few years. Given an increasing clogged communication infrastructure, being able to monitor and maintain the integrity of 3D video streams is of high interest. However, our understanding of the perceptual factors that determine the quality of stereoscopic viewed 3D videos remains limited.

The perceptual quality of a stereoscopically viewed 3D image is the topic of this study, which can be very different from the perceived quality of each 2D image in the stereopair. The additional dimension of depth, along with unwanted side effects induced by geometry or poor stereography, leading to visual discomfort or fatigue, can affect the experience of viewing a stereoscopic image in both positive and negative ways. Conversely, a variety of factors need to be considered when creating 3D content, in order to be able to deliver a pleasant stereoscopic 3D viewing experience [4].

* Corresponding author. Tel.: +1 512 471 2887.
E-mail addresses: mjchen@utexas.edu (M.-J. Chen), ccsu@utexas.edu (C.-C. Su), d-kwon@ti.com (D.-K. Kwon), cormack@psy.utexas.edu (L.K. Cormack), bovik@ece.utexas.edu (A.C. Bovik).

0923-5965/$ - see front matter © 2013 Elsevier B.V. All rights reserved.
http://dx.doi.org/10.1016/j.image.2013.05.006

A considerable amount of research has been conducted on the complex relationship between visual comfort and stereography. Such factor as accommodation-convergence conflicts, the distribution of disparities, binocular mismatches, depth inconsistencies, perceptual and cognitive inconsistencies, and the quality of the images, may all affect the degree of visual comfort experienced when viewing stereoscopic content. Lambooij et al. [5] and Tam et al. [6] provide comprehensive reviews of these topics, and some general rules, such as the *zone of comfortable viewing* [7,8], have been proposed to predict potential visual discomfort, and to guide the production of satisfactory stereo content.

Regarding the visual quality of stereoscopic content, while a number of studies on the perception of distorted stereoscopic and 3D QA models have been conducted, methods for predicting 3D image quality remain limited in capability, and indeed none has been shown to outperform 2D QA models when predicting the quality of stereoscopically viewed 3D images. For example, human studies [9–11] on distorted stereoscopic content have shown that the perceptual quality of stereo content cannot be expressed as simply as the average quality of the left view and the right views.

Research on 3D QA models can be divided into two classes based on whether computed disparity information is considered. The first group directly applies 2D QA model to the 3D QA problem. The methods in [12,13] do not use disparity information and apply 2D QA algorithms to the left and right views independently, then combine (by various means) the two scores into a predicted 3D quality score. The models in this class are based on the hypothesis that the quality of a binocularly viewed image may be deduced from the quality of the 2D images without accessing disparity or the third dimension. However, other studies provide evidence that the quality of stereoscopically viewed images is generally different than a simple combination of the qualities of the 2D viewed images. For example, Meegan et al. [10] claimed that the binocular sense of the quality of asymmetric MPEG-2 distorted stereo images is approximately the average of the quality of the two views, but that the perception of asymmetric blur distorted stereo images is dominated by the higher quality view.

The second class of models takes depth information into account, typically by applying 2D quality assessment (QA) algorithms on both stereo images and also on the estimated disparity map [14–20]. A 3D quality score is then generated using a combination of the various predicted 2D scores. The hypothesis underlying these QA models is that 3D viewing quality is correlated with depth quality. In this direction, Seuntiens [21] coined the term viewing experience to describe the overall sensation of viewing stereoscopic content. This author opines that the quality of a stereoscopic viewing experience is chiefly determined by three factors: image quality, depth quality, and naturalness. However, it is difficult to assess the quality of perceived depth or disparity, since ground truth disparity or depth is generally not available. Such models can only assess the depth quality using estimated disparity maps (computed from a pristine stereopair and/or from a distorted stereopair). Hence 3D QA performance may be substantially affected by the accuracy of the disparity estimation algorithm that is used. Moreover, benchmark tests on stereo algorithms [22] utilize high-quality stereo images, and the performance of stereo algorithms on distorted stereo images is rarely considered.

3D QA models that utilize models of binocular perception are also available. Bensalma et al. [23] proposed a 3D QA algorithm that measures the difference of binocular energy between the reference and tested stereopairs, and thus considers the potential influence of binocularity on perceived 3D quality. However, in their experiment, they only compared the performance of their model with Peak-Singal-to-Noise-Ratio (PSNR) and the Structural SIMilarity (SSIM) index, which perform significantly worse than high performance 2D FR QA models, such as Multi-Scale Structural SIMilarity (MSSSIM) index [24] and visual information fidelity (VIF) [25]. Thus, it is still questionable whether their model can outperform high performance 2D FR QA models in prediction the quality of stereoscopic 3D images. In addition, they only provided performance numbers for JPEG distortion stereo images. Wang et al. [26] proposed a 3D QA model that is based on the suppression theory of binocular fusion. The basic tenet of the suppression theory is that the binocular visual signal is, in fact, a spatial patchwork of monocular inputs. In other words, in any given spatial region, vision is dominated by either one eye or the other. Within this framework, it is conceivable that spatial detail could be carried by one eye's signal, with the other eye contributing only what is necessary for disparity computations. Unfortunately, as summarized in Howard and Rogers [27], a vast body of the literature has rendered the suppression theory untenable. Thus, any QA metric based on the suppression theory cannot be based what the human visual system actually does. Ryu et al. [28] also proposed a 3D FR QA model that utilized research on binocular perception. In their model, the 3D quality score is a weighted summation of the quality scores from the left and right views.

We take steps towards ameliorating some of these shortfalls by introducing a 3D QA framework that is based on biologically plausible visual processing. Our proposed model is motivated by the results of studies on masking and facilitation effects experienced when viewing stereoscopic images. In particular, we make a model of the influence of binocular rivalry between the left-right views. Evidence from a series of directed human studies is shown to support the ideas embodied in this new 3D QA framework. A practical 3D QA algorithm is derived and shown to perform well on a large 3D image quality database containing both symmetric and asymmetric distorted stereopairs equipped with associated ground truth disparity maps.

The reminder of this paper is organized as follows. Section 2 describes related work on relevant aspects of 3D perception which helps to motivate the models that are used. The overall 3D QA framework is described in Section 3 including the derivation of a practical 3D QA algorithm from the models. Section 4 describes the experiments conducted on the 3D QA database and analyzes the model performance. Finally, Section 5 concludes the paper with a discussion of ideas for future work.

2. Distortion perception on stereo images

In order to explain the ideas underline the 3D QA modeling framework, we first review some relevant findings on 3D distortion perception (Section 2.1). We then focus on the highly relevant phenomenon of binocular rivalry (Section 2.2) and how it affects the quality of distorted stereo images.

2.1. Masking/facilitation of distorted stereo images

Meegan et al. [10] founded that the task of conducting subjective 3D QA on MPEG compressed video content can be reduced to conducting 2D spatial QA, but on blur distorted content conducting 2D QA is insufficient. Seuntiens et al. [9] later found similar behavior on JPEG compression distorted images, reinforcing the idea that the impact of 2D distortion on 3D content is highly distortion-dependent.

Of course, the interaction of distortion with content can greatly influence distortion visibility and annoyance level, e.g., the well-known masking effect [30]. However, there exists only a vanishingly small literature on depth/disparity masking, and no prior work on the effect of depth/disparity content on distortion visibility. Thus, to gain insight into possible depth masking or binocular effects of stereo 3D distortions, a study wherein human subjects were asked to identify local distortions embedded in stereopairs was conducted [29]. Fig. 1 illustrates a local distorted stimulus in a 2D image. By varying the position of the local distortion on both views, symmetric and asymmetric distorted stereopair were created. The study design provided both subjective quality ratings and data directly linked to subject performance (success rate and response times when asked to find distortions). Four diverse distortion types were studied: white noise, blur, JPEG compression, and JP2K compression distortions.

Two main observations of use arose from this study. First, we found that the perceived quality of a stereoscopic image cannot be accurately characterized by the average qualities of the left and right images for blur, JPEG, and JP2K distorted stereo images, but that the average may be a good quality predictor for white noise distorted stereo images. Our findings on JPEG distorted images were different than those reported in prior work [9], but are statistically significant. Second, we did not observe any depth masking effect for stereoscopic images, i.e., masking of distortion by depth activity. However, for stereoscopic images distorted by blur, JPEG, or JP2K distortions, we found the surprising opposite: that distortions co-located with high depth variations are more easily found by the human subjects, i.e., there exists a *facilitation effect*.

Fig. 1. Image with local white noise distortion. The boundary was blended using a Gaussian blending window. When the image was presented, the subject was requested to point out the distortion by clicking the mouse cursor on the distortion.

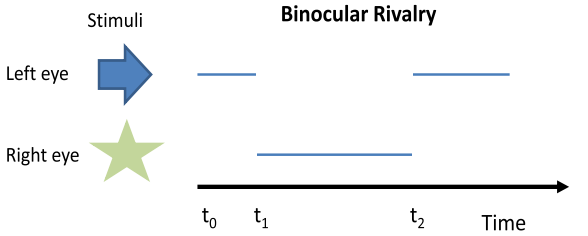

Fig. 2. Illustration of binocular rivalry: Two different stimuli are presented to the left eye (an arrow) and the right eye (a star). The blue line indicates that the stimulus is perceived by a human observer inside that time interval. (For interpretation of the references to color in this figure legend, the reader is referred to the web version of this article.)

Given that the stereoscopically viewed quality of a stereoscopic image cannot generally be accurately predicted by the average qualities of the two stereo images for all distortion types; and that it depends on the type of distortion, then it is sensible to incorporate this observation into a 3D stereoscopic QA model.

2.2. Binocular rivalry

Binocular rivalry is a perceptual effect that occurs when the two eyes view mismatched images at the same retinal location(s). Here, mismatch means that the stimuli received by the two eyes are sufficiently different from each other to cause match failures or to otherwise affect stereoperception. Failures of binocular matching trigger binocular rivalry, which is experienced in various ways, i.e., a sense of failed fusion or a bi-stable alternation between the left and right eye images. Fig. 2 shows an example of binocular rivalry when mismatched stimuli are present. In Fig. 2, in the interval (t_0, t_1), the observer saw the stimulus from the left eye (the arrow). Then, the stimulus from the right eye (the star) dominated until time t_2, after which the observer again saw an arrow. This fluctuation continues when an observer is experiencing binocular rivalry. The fluctuation period may vary from a fraction of a second to several seconds, and it may depend on the color, shape, and texture of the stimuli. Binocular suppression [31] is a special case of binocular rivalry. When binocular suppression[1] is experienced, no rivalrous fluctuations occur between the two images when viewing the mismatched stereo stimulus. Instead, only one of the images is seen while the other is

[1] Binocular suppression does not equal to the suppression theory of binocular fusion used by Wang's work [26].

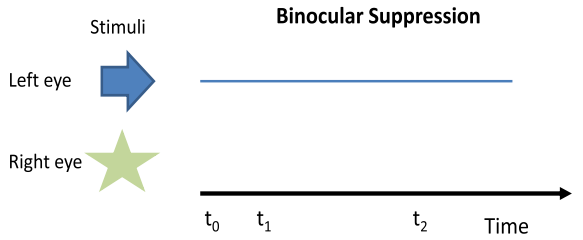

Fig. 3. Illustration of binocular suppression: two different stimuli are presented to the left eye (an arrow) and the right eye (a star). An observer only sees the arrow when s/he experiences binocular suppression.

hidden from conscious awareness. Fig. 3 shows an example of binocular suppression.

Numerous studies have been conducted towards understanding binocular rivalry/suppression. Currently, three different models are prevalent: early suppression, late (high-level) suppression, and a hybrid model including both early and late processes. The early suppression model [32–34,31,35] suggests that binocular rivalry is the result of competition between the eyes. This model views rivalry as an early visual process involving reciprocal inhibition between the monocular channels.

Research that supports a high level suppression model [36,37], on the other hand, argues that there is very little correlation between neural activity and perceptual alternations in area V1 of visual cortex. Moreover, there are some early cortical neurons whose activity is anti-correlated with binocular perception; this means that these neurons fire more when acting on suppressed stimuli. Hence, it has been claimed that the rivalry model should be high-level. For example, Alais and Blake [38] showed that grouping information may contribute to binocular rivalry. Finally, since both early and late models are supported by some evidence, more recent research [39] suggests that a hybrid model may be the best explanation. However, these ideas have not previously been applied towards understanding how binocular rivalry might be related to distortion type. Another important finding is that binocular rivalry is a nearly independent local process. A series of papers [40,41,38] discuss whether the binocular rivalry zones function independently, and their findings indicate that binocular rivalry is composed of local processes.

The discussions in Section 2 provide basic concepts that are used in the 3D QA framework that is introduced in the next section.

3. A framework for quality assessment of distorted stereo images

The logical goal of a 3D stereoscopic QA model is to estimate the quality of the true cyclopean image formed within an observer's mind when a stereo image pair is stereoscopically presented. Of course, simulating the true *cyclopean* image [42] associated with a given stereopair is a daunting task, since it would require accounting for the display geometry, the presumed fixation, vergence, and accommodation. This task is herculean, and is compounded by the fact that it is still unclear how a true

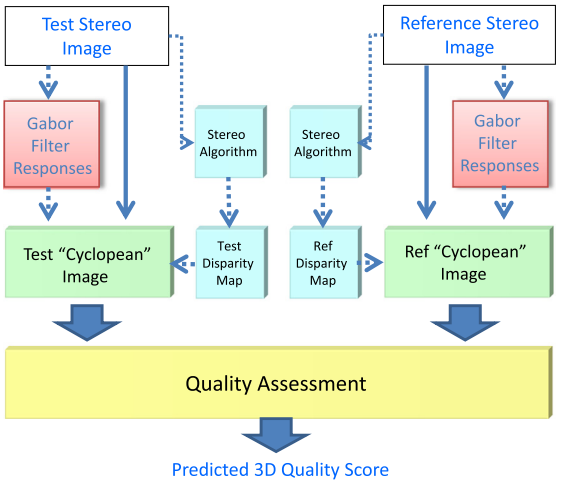

Fig. 4. The proposed framework for 3D quality assessment.

cyclopean image is formed! Towards a limited approximation of this goal, however, we seek to synthesize an internal image having a quality level that is close to the quality of the true *cyclopean* image. By way of notation, henceforth we still use the term "cyclopean" image to represent the synthesized image and *cyclopean* image to mean the one formed in the observer's mind. By performing 3D quality assessment on the synthesized "cyclopean" image we hope to produce accurate estimates of 3D quality perceived on the true *cyclopean* image.

The concept underneath the model framework is shown in Fig. 4. Given a stereo image, an estimated disparity map is generated by a stereo algorithm, while Gabor filter responses are generated on the stereo images using a bandpass filter bank. A cyclopean image is synthesized from the stereo image pair, the estimated disparity map, and the Gabor filter responses. A cyclopean image is created from the reference stereopair and another "cyclopean" image is calculated from the test stereopair. Finally, full reference 2D QA models are applied to the two cyclopean images to predict 3D quality scores.

3.1. Disparity estimation

Research on stereo algorithm (disparity estimation) design has been a topic of intense inquiry for decades. However, there is no consensus on the type of stereo matching algorithm that should be used in 3D QA other than it be of low complexity. Further, there is scarce literature on the performance of stereo algorithms operating under different distortion regimens. Therefore, we deploy a variety of these efficient stereo depth-finding algorithms differing considerably in their operational constants along with the framework we described above to assess perceived 3D quality.

In order gain insights into the influence of stereo algorithms on the performance of 3D QA models, three stereo algorithms were selected based on their complexity and performance. In general, better stereo algorithms (based on results on the Middlebury database [22]) have higher computational complexity, and we balanced this

tradeoff in the choice of stereo matching models. The first algorithm has the lowest complexity. It uses a very simple sum-of-absolute difference (SAD) luminance matching functional without a smoothness constraint. The disparity value of a pixel in a stereopair is uniquely computed by minimizing the SAD between this pixel and its horizontal shifted pixels in the other view with ties broken by selecting the lower disparity solution. The second algorithm [43] has the highest complexity among the three models. This segmentation-based stereo algorithm delivers highly competitive results on the Middlebury database [22]. The third is a SSIM based stereo algorithm that uses SSIM scores to choose the best matches. The disparity map of a stereopair is generated by maximizing the SSIM scores between the stereopair along the horizontal direction, again resolving ties by a minimum disparity criterion.

3.2. Gabor filter bank

As discussed earlier, when the two images of a stereopair present different degrees or characteristics of distortion, the subjective quality of the stereoscopically viewed 3D image generally cannot be predicted from the average quality of the two individual images. Binocular rivalry is a reasonable explanation for this observation. Levelt [34] conducted a series of experiments that clearly demonstrated that binocular rivalry/suppression was strongly governed by low-level sensory factors. He used the term stimulus strength, and noted that stimuli that were higher in contrast, or had more contours, tend to dominate the rivalry. Inspired by this result, we use the energy of Gabor filter bank responses on the left and right images to model stimulus strength and to simulate rivalrous selection of "cyclopean" image quality.

The Gabor filter bank extracts features from the luminance and chrominance channels. These filters closely model frequency-orientation decompositions in primary visual cortex and capture energy in a highly localized manner in both space and frequency [44]. A complex 2D Gabor filter is defined

$$G(x,y,\sigma_x,\sigma_y,\zeta_x,\zeta_y,\theta) = \frac{1}{2\pi\sigma_x\sigma_y} e^{-(1/2)[(R_1/\sigma_x)^2+(R_2/\sigma_y)^2]} e^{i(x\zeta_x+y\zeta_y)} \quad (1)$$

where $R_1 = x\cos\theta + y\sin\theta$, and $R_2 = -\sin\theta + y\cos\theta$, σ_x and σ_y are the standard deviations of an elliptical Gaussian envelope along x and y axes, and ζ_x and ζ_y are spatial frequencies, and θ orients the filter. The design of the Gabor filter bank was based on the work conducted by Su et al. [45]. The local energy is estimated by summing Gabor filter magnitude responses over four orientations (horizontal, both diagonals, and vertical (90°) at a spatial frequency of 3.67 cycles/degree, under the viewing model described in Section 4.1.3.

Regarding the choice of the spatial center frequency, Tyler [46] pointed out that the depth signal in human vision is carried within a much smaller band-width than is the luminance channel. In addition, Schor et al. [47] found that the stereoacuity of human vision normally falls off quickly when seeing stimuli dominated by spatial frequencies lower than 2.4 cycles/degree. Based on their findings, using filters having spatial center frequencies in the range from 2.4 to 4 cycles/degree should produce responses to which a human observer would be most sensitive.

3.3. Cyclopean image

A linear model was proposed by Levelt [34] to explain the experience of *binocular rivalry* in perceived *cyclopean* image when a stereo stimulus is presented. The model he proposed is

$$w_l E_l + w_r E_r = C \quad (2)$$

where E_l and E_r are the stimuli to the left and the right eye respectively, w_l and w_r are weighting coefficients for the left and right eye that are used to describe the process of binocular rivalry, where $w_l + w_r = 1$, and C is the *cyclopean* image.

Given that a foveally presented monocular stimulus generally does not disappear spontaneously, he hypothesized that the duration of a period of dominance period of an eye does not depend on the strength of the stimulus presented to that eye, but rather on the stimulus strength presented to the other eye. Therefore, he concludes that the experience of binocular rivalry is not correlated to the absolute stimulus strength of each view, but is instead related to the relative stimulus strengths of two views. He also proposed a model whereby the weighting coefficients are positively correlated with the stimulus strengths, which we embody in a biologically plausible model whereby the local energies of the responses of a bank of Gabor filters are used to weight the left and right image stimuli. Since binocular rivalry is a local multiscale phenomena (as discussed in Section 2.2), broadening Levelts model in this manner is a natural way to simulate a synthesized cyclopean image. In our model, as in Levelts; the stereo views used to synthesize to the cyclopean view are disparity-compensated then the "cyclopean" image is mapped onto the coordinate system of the left view image. Thus the localized linear model that we use to synthesize a "cyclopean" image is

$$CI(x,y) = W_L(x,y) \times I_L(x,y) + W_R((x+d),y) \times I_R((x+d),y) \quad (3)$$

where CI is the simulated "cyclopean" image, I_L and I_R are the left and right images respectively, and d is a disparity index that corresponds pixels from I_L to those in I_R. The weights W_L and W_R are computed from the normalized Gabor filter magnitude responses

$$W_L(x,y) = \frac{GE_L(x,y)}{GE_L(x,y) + GE_R((x+d),y)} \quad (4)$$

$$W_R(x+d,y) = \frac{GE_R((x+d),y)}{GE_L(x,y) + GE_R((x+d),y)} \quad (5)$$

where GE_L and GE_R are the summation of the convolution responses of the left and right images to filters of the form (1). Because of the normalization in (5), increased Gabor energy of either (the left or right) stimulus suppresses the contribution of the other view when there is binocular rivalry. Finally, the task of 3D QA is performed by applying

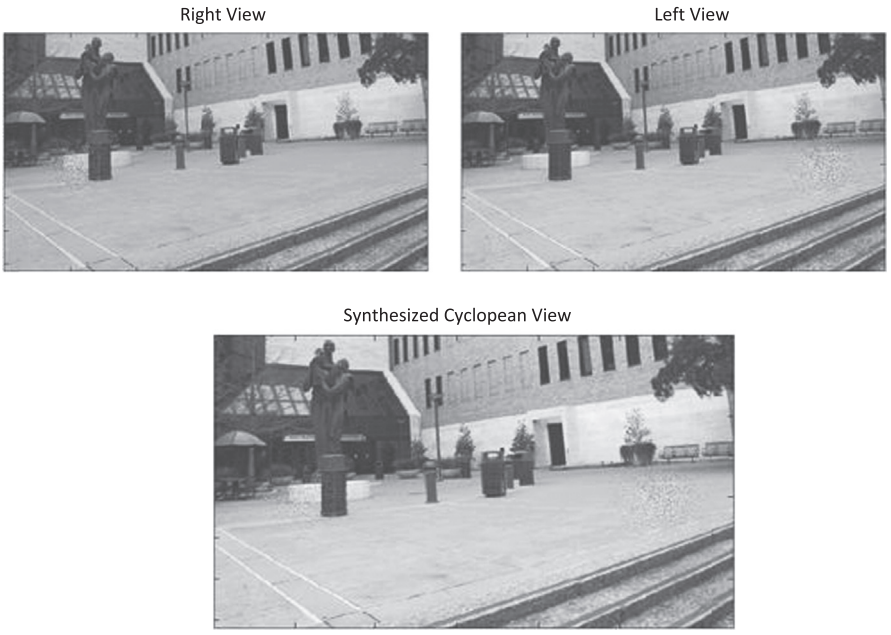

Fig. 5. Top: stereo images with local white noise distortion. Bottom: cyclopean image synthesized by the proposed framework.

a full reference 2D QA algorithm on the reference "cyclopean" image and on the test "cyclopean" image.

Fig. 5 shows an example of a synthesized "cyclopean" image. The stereopairs in Fig. 5 are locally distorted by white noise patches at different locations. Since the white noise distortion produces a elevated stimulus strength, the synthesized cyclopean image is dominated by white noise distortion, which approximates the experience when stereoscopically viewing the stereopair.

4. Experiment and discussion

A human study was conducted to construct a subjective data set to be used in assessing algorithms of this type. This section describes the human study and experiments performed using it.

4.1. Stereoscopic image quality dataset

A stereoscopic image quality dataset annotated with associated subjective quality ratings was constructed using the outcomes of a human study. The details of the dataset and human study are described in the following.

4.1.1. Source images

The stereo images used for the study were captured by members of the LIVE lab. They captured co-registered stereo images and range data with a high-performance range scanner (RIEGL VZ-400 [48]) with a Nikon D700 digital camera mounted on the top. The stereo images pairs were shot with a 65 mm camera base distances. Off-line correction was later applied to deal with translations occurring during capture. The sizes of the images are 640×360 pixels. The eight pristine images are shown in Fig. 6, while Fig. 7 shows the ground truth depth map of one of them. The eight pairs of stereo images to be used in this study were taken on the campus of The University of Texas at Austin and a nearby park. The ground truth depth map of each stereopair was transformed to a ground truth disparity map based on the captured model described above.

4.1.2. Participants

Six females and twenty-seven males participated in the experiment all aged between 22 and 42 years. A Randot stereo test was used to pre-screen participants for normal stereo vision. Each subject reported normal or corrected normal vision and no acuity or color test was deemed necessary.

4.1.3. Display setting

The study was conducted using a Panasonic 58 in. 3D TV with active shutter glasses. The viewing distance was set at 116 in., which is four times the screen height.

4.1.4. Stimuli

Both symmetric and asymmetric distortions were generated. The distortions that were simulated include compression using the JPEG and JP2K compression standards, additive white Gaussian noise, Gaussian blur and a fast-fading model based on the Rayleigh fading channel. The degradation of stimuli was varied by control parameters within pre-defined ranges; the control parameters are reported in Table 1. The ranges of control parameters were decided beforehand to ensure that the distortions varied from almost invisible to severely distorted with good overall perceptual separation. For each distortion type, every reference stereopair was distorted to create three symmetric distorted stereopairs and six asymmetric distorted stereopairs. Thus, a total of 360 distorted stereopairs were created.

Fig. 6. The eight reference images (only left views are shown) used in the experiment.

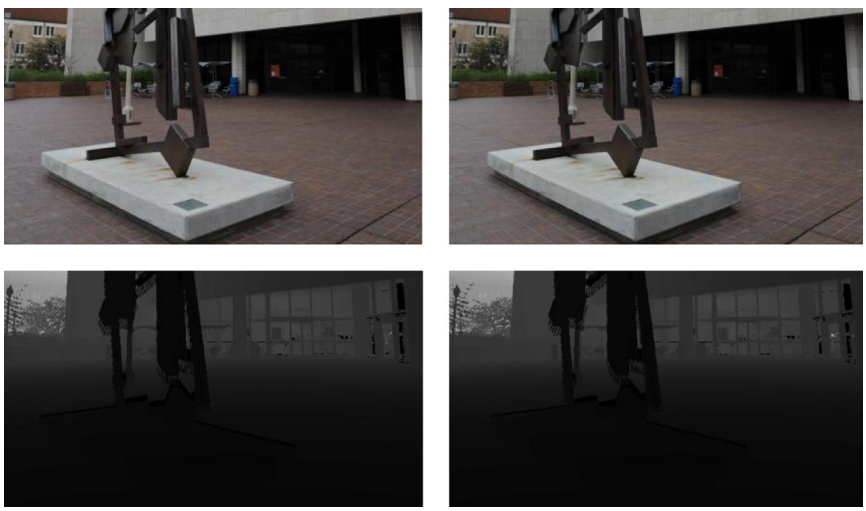

Fig. 7. A stereo image (free-fuse the left and right images) and the ground truth disparity maps.

Table 1
Range of parameter values for distortion simulation.

Distortion	Control parameter	Range
WN	Variance of Gaussian	[0.001 0.5]
Blur	Variance of Gaussian	[0.5 30]
JP2K	Bit-rate	[0.04 0.5]
JPEG	Quality parameter	[8 50]
FF	Channel signal-to-noise ratio	[15 30]

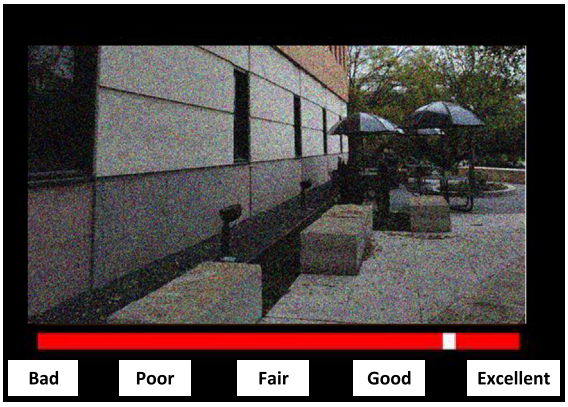

Fig. 8. Illustration with 2D image, the study was conducted with 3D stimuli. The subject was requested to give a overall 3D viewing experience when a 3D stimulus is shown.

4.1.5. Procedure

We followed the recommendation for a single stimulus continuous quality scale (SSCQS) [49] to collect the 3D subjective image quality of each distorted stereoscopic image. The instructions given to each participant was: give an overall rating based on your viewing experience when viewing the stereoscopic stimuli. The ratings were obtained on a continuous scale labeled by equally spaced adjective terms: bad, poor, fair, good, and excellent, i.e. a Liekart scale. The graphic user Interface (GUI) used is shown in Fig. 8. The experiment was divided into two sessions; each held to less than 30 min to minimize subject fatigue. A training session using six stimuli was conducted before the beginning of each study to verify that the participants were comfortable with the 3D display and to help familiarize them with the user interface used in the task. The training content was different from the images in the study and was impaired using the same distortions. Questions about the experiment were answered during the training session and a short post-interview was conducted to determine whether the participant experienced visual discomfort during the experiment. Only two participants reported any visual discomfort.

4.1.6. Subjective quality scores

Difference opinion scores (DOS) were obtaining by subtracting the ratings that the subject gave each reference stimuli from the ratings that the subjective gave to the corresponding test distorted stimuli. The remaining subjective scores were then normalized to Z-scores, and then averaged across subjects to produce difference mean opinion scores (DMOS).

4.2. Performance against subjective quality ratings

We studied four widely-used full-reference 2D QA metrics (PSNR, SSIM [50], VIF [51] [43], and MS-SSIM candidate 2D QA methods to be used within the 3D QA framework. This is the final stage of predicting the quality of the *cyclopean* image. We used Spearman's rank ordered correlation coefficient (SROCC), the linear (Pearson's) correlation coefficient (LCC) and the root-mean-squared error (RMSE) to measure the performance of the 3D QA models thus devised. LCC and RMSE were computed after logistic regression through a non-linearity which is described in [25]. Higher SROCC and LCC values indicate good correlation (monotonicity and accuracy) with human quality judgments, while lower values of RMSE indicate better performance.

4.2.1. Performance using ground truth disparity map

We begin the performance analysis by using ground truth depth, which minimizes the effects of flaws in the stereo matching algorithms. The performance numbers are shown in Tables 2–4. Also included are the performance numbers arrived at using the same 2D FR QA algorithms, simply applied to the left and right views and the QA scores averaged. The "cyclopean" QA algorithm does significantly better than the 2D baseline QA algorithms on the mixed data set containing both symmetric and asymmetric distorted data.

Table 2
SROCC scores obtained by averaging left and right QA scores (center column) and using the 3D "cyclopean" model (right column).

Algorithm	2D baseline	"Cyclopean model"
PSNR	0.672	0.762
SSIM	0.796	0.856
MS-SSIM	0.78	**0.901**
VIF	0.822	0.864

Table 3
LCC scores obtained by averaging left and right QA scores (center column) and using the 3D "cyclopean" model (right column).

Algorithm	2D baseline	"Cyclopean model"
PSNR	0.687	0.783
SSIM	0.804	0.867
MS-SSIM	0.784	**0.908**
VIF	0.844	0.872

Table 4
RMSE values obtained by averaging left and right QA scores (center column) and using the 3D "cyclopean" model (right column).

Algorithm	2D baseline	"Cyclopean model"
PSNR	17.67	15.09
SSIM	14.43	12.11
MS-SSIM	15.09	**10.2**
VIF	13.03	11.89

It is clear from Tables 2 to 4 that MS-SSIM delivers the best performance among the four 2D QA algorithms when embedded in the "cyclopean" model. Fig. 9 breaks down the performance of the "cyclopean" model using MS-SSIM. Clearly, the QA performance is improved on blur and JP2K as might be expected, since strong binocular rivalry exists in asymmetric blur and JP2K distorted stereo images. The improvement in QA performance for FF distorted images is also significant for similar reasons. For stereo images distorted by white noise, there is no significant difference between the performance of averaged 2D QA and the "cyclopean" mode since binocular rivalry does not occur in white noise distorted stereo images [29]. For JPEG compression distorted stereo images, the performance numbers of the averaged 2D QA and the "cyclopean" model are very close. These results strongly suggest that binocular rivalry is an important ingredient in subjective stereoscopic QA, and our "cyclopean" framework successfully captures and utilizes binocular rivalry to predict subjective 3D quality. Fig. 10 plots the predicted quality scores using MS-SSIM (after logistic regression) versus DMOS. Predicted scores from the proposed "cyclopean" framework are shown on top-left, while the bottom-left plot shows the scores from the 2D baseline. Clearly, the predicted scores attained using the "cyclopean" framework are better than the scores predicted by the 2D baseline. Moreover, the predicting errors which are measured by root mean square error (RMSE) of the "cyclopean" framework are lower than the predicting errors of the 2D baseline.

To obtain deeper insights into how the performance of the "cyclopean" 3D QA model is improved by accounting for

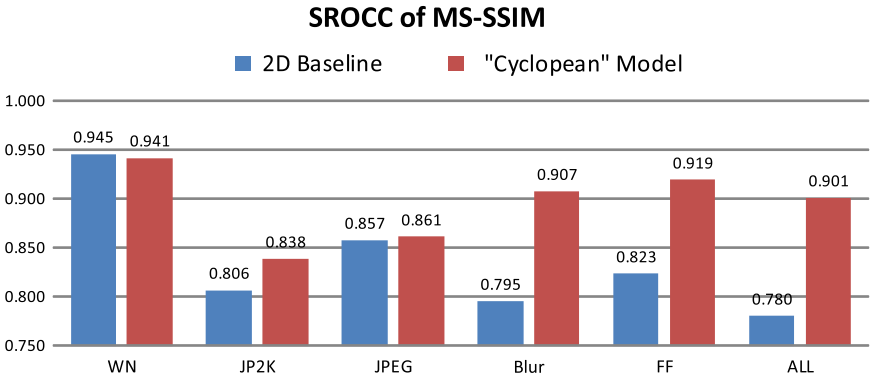

Fig. 9. SROCC values using MS-SSIM, broken down by distortion type.

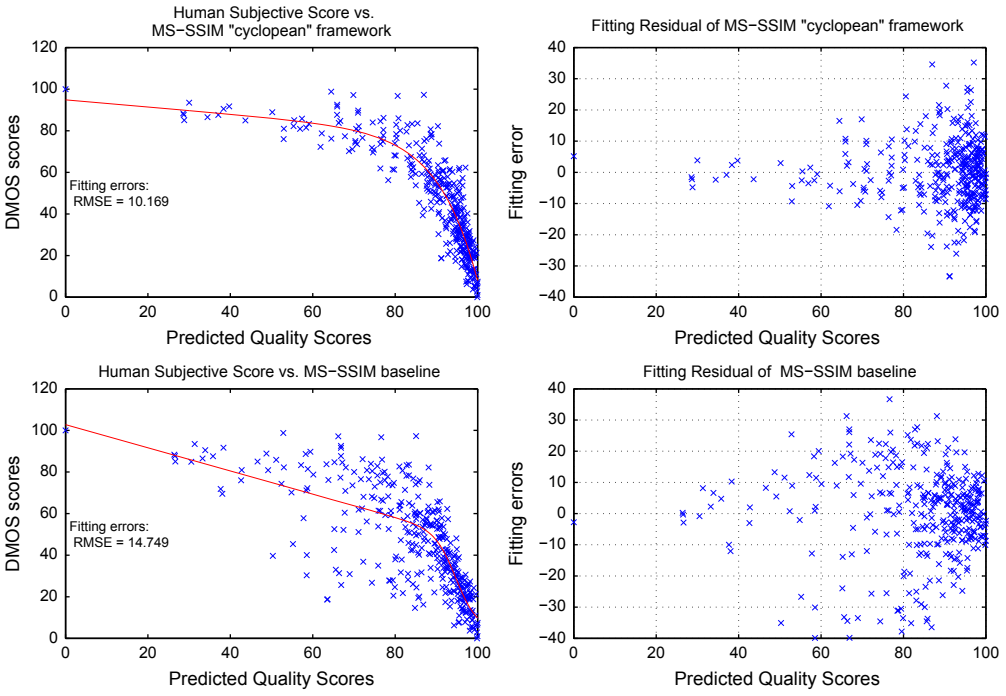

Fig. 10. Plot of predicted objective scores versus DMOS and predicting errors. Top left: predicted by MS-SSIM "cyclopean" framework. Top right: predicting errors of MS-SSIM "cyclopean" framework. Bottom left: predicted by MS-SSIM 2D baseline. Bottom right: predicting errors of MS-SSIM 2D baseline.

binocular rivalry, its performance on the separated symmetric and asymmetric distorted stereopairs is reported in Tables 5–7. The performance numbers in Tables 5–7 indicate that the "cyclopean" model did not boost performance on symmetric distorted stereoscopic images. However, performance was greatly enhanced on the asymmetric distorted stereopairs. Furthermore, Tables 5–7 indicate that the task of predicting the quality of asymmetric distorted stereopairs is more difficult than that of predicting the quality of symmetric distorted data.

4.2.2. Influence of stereo matching algorithms

The preceding discussion describing the stereoscopic "cyclopean" QA model assumed that highly accurate ground truth depth values are available. Next, we study stereoscopic QA performance when estimated depth is used as computed by stereo algorithms.

Currently, stereo matching algorithms are generally tested on undistorted stereo images and compared using a simple measure (bad-pixel rate) [22]. The bad-pixel rate (BR) is defined as

$$BR = \frac{1}{N}\sum_{(x,y)} |d_C(x,y) - d_T(x,y)| > \delta_d \quad (6)$$

where δ_d is a disparity error tolerance, d_C is the computed disparity map, and d_T is a ground truth depth map. We use $\delta_d = 1$ as suggested by the authors of [22].

However, we believe that such metrics provide little or no information regarding perceived 3D image quality. Indeed, there have been no studies conducted to determine the degree to which the quality of an estimated disparity map is correlated with subjective judgements of depth. It is likewise unclear whether distortions of stereopairs affects perceived depth quality [11,21].

The bad-pixel rates of the three selected stereo algorithms against ground truth are reported in Table 8. Clearly, all perform equally poorly when applied to distorted images. This lack of robustness is not unexpected owing to the ill-posedness of the stereo problem, and since none of these (or any other) stereo algorithms has been designed to excel in the presence of distortions. For example, as shown in Fig. 11, white noise confuses the SSIM-based stereo matching algorithm, yet a human observer easily fuses the stereopair. In addition, the ground truth maps that we used were obtained using a high-resolution laser range scanner. The ground truth maps have relatively fine disparity resolution over both smooth and depth-textured regions.

Next, we discuss the influence of poor disparity estimation performance on 3D stereo QA. The performance of the "cyclopean" model using ground truth disparity, estimated disparity, and no disparity information are reported in Table 9. Table 9 shows that there is no significant difference in the performance attained using the ground truth and estimated disparities, although the performance of the very simple SAD-based stereo algorithm is slightly lower than the other two stereo algorithms. All three significantly outperform the no-disparity case indicating that estimated disparities provide useful information when predicting the quality of the stereo 3D images in the database. These results suggest that we should not use bad-pixel rate to evaluate stereo algorithms in the context of 3D image quality assessment algorithm design. Note that the depth signal in human vision occupies a much narrower bandwidths than the luminance spatial channel [52–54], suggesting that a low-resolution disparity map maybe adequate for the task of 3D quality assessment.

4.2.3. Comparison with existing 3D QA models

Gorley and Holliman [13] proposed a PSNR-based 3D stereo QA model that does not include depth. Benoit et al. [15] proposed a SSIM-based stereo QA model operating on both stereopairs and disparity maps. You et al. [19] applied

Table 5
SROCC scores relative to human subjective scores. Obtained using averaged left-right QA scores (2D baseline) and the "cyclopean" model on symmetric and asymmetric distorted stereopairs.

	Symmetric		Asymmetric	
	2D baseline	"Cyclopean" model	2D baseline	"Cyclopean" model
PSNR	0.781	0.819	0.596	0.698
SSIM	0.826	0.85	0.742	0.827
MSSSIM	0.912	0.929	0.687	0.854
VIF	0.916	0.902	0.737	0.804

Table 6
LCC scores relative to human subjective scores obtained using averaged left-right QA scores (2D baseline) and the "cyclopean" model on symmetric and asymmetric distorted stereopairs.

	Symmetric		Asymmetric	
	2D baseline	"Cyclopean" model	2D baseline	"Cyclopean" model
PSNR	0.791	0.825	0.625	0.737
SSIM	0.845	0.882	0.767	0.850
MSSSIM	0.924	0.937	0.709	0.879
VIF	0.924	0.906	0.772	0.822

Table 7
Fitting errors measured by RMSE obtained using averaged left-right QA scores (2D baseline) and the "cyclopean" model on symmetric and asymmetric distorted stereopairs.

	Symmetric		Asymmetric	
	2D baseline	"Cyclopean" model	2D baseline	"Cyclopean" model
PSNR	16.42	15.15	16.83	14.58
SSIM	14.35	12.65	13.85	11.37
MSSSIM	10.23	9.37	15.20	10.29
VIF	10.23	11.35	13.69	12.27

Table 8
Mean bad pixel rate value on 360 distorted stereopairs with standard deviation (inside the bracket) for three stereo algorithms.

	SAD	SSIM	Klaus
Bad-pixel rate	79.8% (9.24)	79.52% (10.7)	78.04% (11.83)

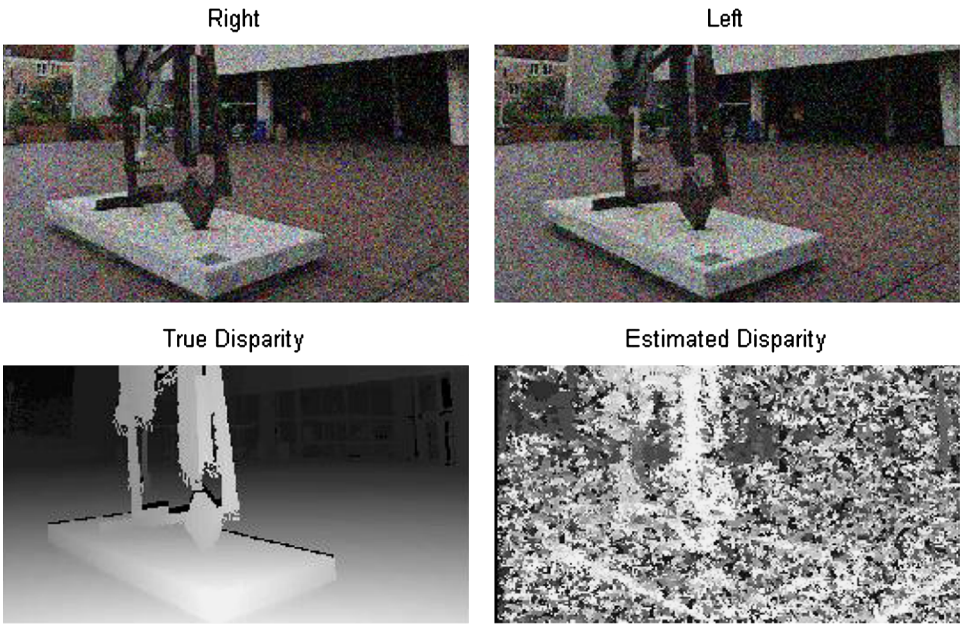

Fig. 11. Depth estimation using SSIM-based stereo algorithm on noised distorted stereo pairs. Free-fuse the noisy stereo image to see a 3D image.

Table 9
SROCC, LCC, and RMSE relative to human subjective scores attained by "cyclopean" model using disparity maps computed using different stereo algorithms.

Stereo algorithm	SROCC	LCC	RMSE
Ground truth	0.901	0.907	10.2
SAD	0.876	0.885	11.29
SSIM	0.893	0.901	10.58
Klaus	0.890	0.896	10.80
No depth information	0.817	0.824	13.73

Table 10
SROCC, LCC, and RMSE relative to human subjective scores attained by several 3D QA models using SSIM-based stereo algorithm.

Algorithm	SROCC	LCC	RMSE
Proposed (MS-SSIM)	0.893	0.901	10.58
Baseline (MS-SSIM)	0.780	0.784	15.09
Benoit [15]	0.728	0.745	16.2
You [19]	0.784	0.797	14.66
Hewage [17]	0.496	0.55	20.29
Gorley [13]	0.158	0.511	20.88

a variety of 2D QA models on stereopairs and disparity map and tried a number of ways to combine the predicted quality scores from stereopairs and disparity maps into predicted quality scores. Their best result is also SSIM-based. Hewage and Martini [17] proposed a PSNR-based reduced-reference stereo quality model utilizing disparity. In our simulations, since some of these algorithms require estimated disparity maps from both reference and test stereopairs, we used the SSIM-based stereo algorithm to create disparity maps.

Table 10 shows the performances of these 3D QA algorithms as compared with the "cyclopean" model. The "cyclopean" model using MS-SSIM delivers the highest performance, followed by the model proposed by You et al., which yields no significant difference relative to the performance of left-right averaged 2D QA using MS-SSIM. The performances of the other three algorithms are lower than this 2D baseline. This is another powerful demonstration of the importance of accounting for binocular rivalry when conducting stereoscopic QA.

4.2.4. Testing with other 3D image dataset

To the best of our knowledge, the number of publicly available stereo 3D image quality dataset is very limited [15,18,55]. Among these three datasets, only the MICT stereo image database [18] includes asymmetrically distorted stereo images. However, the MICT database is comprised only of distorted stereo images and the ground truth disparity maps are not available. The MICT stereo image database has 480 JPEG distorted stereo images and 10 pristine stereo images. The distorted stereo images include both asymmetrically and symmetrically JPEG distorted stereo images. However, a double stimulus impairment scale (DSIS) protocol and a discrete scale were used in the subjective study. Subjects were asked to assess the annoyance they experienced when viewing each distorted stereo image pair against the simultaneously displayed reference image by choosing a rating among the following five options: 5=imperceptible, 4=perceptible but not annoying, 3=slightly annoying, 2=annoying and 1=very annoying. The display they used was a very small (10-in.) auto-stereoscopic display, and the viewing distance was not provided.

The performance numbers (SROCC, LCC, and MSE) of 2D and 3D QA models on the MICT database are shown in Table 11. From Table 11, it is clear that the 2D FR model MS-SSIM delivers the best performance among all the compared QA models on the MICT dataset. Neither our cyclopean model nor other 3D QA models outperforms 2D

Table 11
Performance numbers tested against MICT database. Italicized algorithms are 2D IQA algorithm, others are 3D IQA algorithms.

Algorithm	SROCC	LCC	MSE
2D PSNR	0.586	0.554	0.971
2D SSIM	0.846	0.862	0.591
2D MS-SSIM	0.935	0.935	0.415
Benoit	0.902	0.910	0.483
You	0.857	0.864	0.586
Gorley	0.065	−0.022	1.166
Hewage	0.625	0.623	0.912
Cyclopean MS-SSIM	0.862	0.864	0.587

MS-SSIM on the MICT dataset. The discrepancy between the experimental results of our dataset and the results of the MICT dataset may be caused by the poor performance of disparity estimation algorithm or on the design or environment of the human study. However, further clarification is not feasible unless the ground truth disparity maps of the MICT dataset become available.

5. Conclusion and future work

We presented a new framework for conducting automatic objective 3D QA that delivers highly competitive performance, with a clear advantage when left-right distortion asymmetries are present. The design of the framework is motivated by studies on the perception of distorted stereoscopic images, and recent theories of binocular rivalry. The "cyclopean" 3D QA model that we derived was tested on the LIVE Asymmetric 3D Image Quality Database, and found to significantly outperform conventional 2D QA models and well-known 3D QA models. The impact of the stereo algorithm used to conduct 3D QA was also discussed. We also found that a low-complexity SSIM-based stereo algorithm performs quite well for estimating disparity in the "cyclopean" algorithm in the sense that a high level of 3D QA performance is maintained.

An important contribution of this work is the demonstration that accounting for binocular rivalry can greatly improve the performance of 3D QA models. Indeed, most of the advantage conveyed by the "cyclopean" model was observed on asymmetric distorted stereopairs. The framework can, therefore, ostensibly be used to evaluate the quality of stereo content that has been compressed using a mixed resolution coding technique [56,57]. Compressed stereo content that is transmitted over the wireless Internet may be subjected to other asymmetric distortions as well.

To further advance the performance of current 3D QA models, we think that the effect of depth masking and depth quality needs to be further studied and addressed. Regarding depth masking, our prior work [29] revealed no depth masking effect when viewing distorted stereopairs. However, we do not regard the results of our prior study to be universal and there remain other distortions to be studied. Furthermore, while we did not find depth masking of distortions, we did find evidence of facilitation which may prove relevant to 3D QA.

Regarding the role of computed disparity, prior models utilizing disparity maps derived from reference and test stereopairs have generally failed to deliver better QA performance than 2D QA models on the individual stereo images. Of course, the disparity cue is not the only one used by the human visual system to perceive depth. For example, monocular cues such as occlusion, relative size, texture gradient, perspective distortion, lighting, shading, and motion parallax [58] all affect the perception of depth. It is not yet clear how the brain integrates all these cues to produce an overall sensation of depth [59].

The influences of distortions on perceived depth quality also remain an open question. While Seuntiens et al. [9] claimed that JPEG encoding has no effect on perceived depth, other recent research suggested that perceived depth quality is affected by both blur and white noise distortion, although the influence of distortion on perceived depth is less than the influence on perceived image quality [60]. Another recent study showed that, when viewing stereoscopic videos compressed by an H.264/AVC encoder using a range of QP values, perceived depth quality remained constant for some subjects, but varied with perceived image quality [61] for others. Subject agreement on perceived depth quality was much lower than on perceived image quality. Clearly, more research is merited on how perceived depth quality is affected by different distortion types, and on what kinds of depth cues are most strongly correlated with the reduced quality of depth perception when viewing distorted stereopairs.

References

[1] C. Wheatstone, Contributions to the physiology of vision. Part the first. On some remarkable, and hitherto unobserved phenomena of binocular vision, Philosophical Transactions of the Royal Society of London 128 (1838) 371–394.
[2] List of 3D Movies. URL ⟨http://en.wikipedia.org/wiki/List_of_3-D_films⟩.
[3] ESPN, ESPN 3D Broadcasting Schedule. URL ⟨http://espn.go.com/3d/schedule.html⟩.
[4] S.J. Daly, R.T. Held, D.M. Hoffman, Perceptual issues in stereoscopic signal processing, IEEE Transactions on Broadcasting 57 (2) (2011) 347–361.
[5] M.T.M. Lambooij, W.A. Ijsselsteijn, I. Heynderickx, Visual discomfort in stereoscopic displays: a review, Proceedings of SPIE 6490 (2007) 17.
[6] W.J. Tam, F. Speranza, S. Yano, K. Shimono, H. Ono, Stereoscopic 3D-TV: visual comfort, IEEE Transactions on Broadcasting 57 (2) (2011) 335–346.
[7] N.A. Valius, Stereoscopy, Focal P., New York, London, 1966.
[8] T. Shibata, J. Kim, D.M. Hoffman, M.S. Banks, The zone of comfort: predicting visual discomfort with stereo displays, Vision 11 (8) (2011) 1–29.
[9] P. Seuntiens, L. Meesters, W. Ijsselsteijn, Perceived quality of compressed stereoscopic images: effects of symmetric and asymmetric JPEG coding and camera separation, ACM Transactions on Applied Perception 3 (2) (2006) 95–109.
[10] D.V. Meegan, L.B. Stelmach, W.J. Tam, Unequal weighting of monocular inputs in binocular combination: implications for the compression of stereoscopic imagery, Journal of Experimental Psychology: Applied 7 (2001) 143–153.
[11] W.J. Tam, L.B. Stelmach, P.J. Corriveau, Psychovisual aspects of viewing stereoscopic video sequences [3295–32], Proceedings of SPIE (3295) (1998) 226–235.
[12] S.L.P. Yasakethu, C.T.E.R. Hewage, W.A.C. Fernando, A.M. Kondoz, Quality analysis for 3D video using 2D video quality models, IEEE Transactions on Consumer Electronics 54 (4) (2008) 1969–1976.
[13] P. Gorley, N. Holliman, Stereoscopic image quality metrics and compression, Proceedings of SPIE 6803 (2008) 05.
[14] Z. Zhu, Y. Wang, Perceptual distortion metric for stereo video quality evaluation, WSEAS Transactions on Signal Processing 5 (7) (2009) 241–250.
[15] A. Benoit, P. Le Callet, P. Campisi, R. Cousseau, Quality assessment of stereoscopic images, EURASIP Journal on Image and Video Processing 2008 (2009) 1–13.

[16] Y. Jiachen, H. Chunping, Z. Yuan, Z. Zhuoyun, G. Jichang, Objective quality assessment method of stereo images, in: 3DTV Conference: The True Vision—Capture, Transmission and Display of 3D Video, 2009, pp. 1–4.
[17] C. Hewage, M. Martini, Reduced-reference quality metric for 3D depth map transmission, in: 3DTV Conference: The True Vision—Capture, Transmission and Display of 3D Video, 2010, pp. 1–4, doi: http://dx.doi.org/10.1109/3DTV.2010.5506205.
[18] R. Akhter, J. Baltes, Z. M. Parvez Sazzad, Y. Horita, No-reference stereoscopic image quality assessment, Proceedings of Proc. SPIE 7524, Stereoscopic Displays and Applications XXI, 75240T (February 24, 2010); http://dx.doi.org/10.1117/12.838775.
[19] J. You, L. Xing, A. Perkis, X. Wang, Perceptual Quality Assessment for Stereoscopic Images Based on 2D Image Quality Metrics and Disparity Analysis, 2010.
[20] A. Maalouf, M.-C. Larabi, Cyclop: A stereo color image quality assessment metric, in: IEEE International Conference on Acoustics, Speech and Signal Processing, 2011, pp. 1161–1164.
[21] P. Seuntiens, Visual Experience of 3D TV, 2006.
[22] D. Scharstein, R. Szeliski, A taxonomy and evaluation of dense two-frame stereo correspondence algorithms, International Journal of Computer Vision 47 (2002) 7–42.
[23] R. Bensalma, M.-C. Larabi, A perceptual metric for stereoscopic image quality assessment based on the binocular energy, Multi-dimensional Systems and Signal Processing (2012) 1–36.
[24] Z. Wang, E.P. Simoncelli, A.C. Bovik, Multiscale structural similarity for image quality assessment, in: Asilomar Conference on Signals, Systems and Computers, vol. 2, 2003, pp. 1398–1402.
[25] H. Sheikh, M. Sabir, A. Bovik, A statistical evaluation of recent full reference image quality assessment algorithms, IEEE Transactions on Image Processing 15 (11) (2006) 3440–3451, http://dx.doi.org/10.1109/TIP.2006.881959.
[26] X. Wang, S. Kwong, Y. Zhang, Considering binocular spatial sensitivity in stereoscopic image quality assessment, in: Visual Communications and Image Processing (VCIP), 2011, pp. 1–4, doi:http://dx.doi.org/10.1109/VCIP.2011.6116015.
[27] P. Ian Howard, B.J. Rogers, Binocular Vision and Stereopsis, Oxford University Press, 1995.
[28] S. Ryu, D.-H. Kim, K. Sohn, Stereoscopic image quality metric based on binocular perception model, in: IEEE International Conference on Image Processing.
[29] M.-J. Chen, A.C. Bovik, L.K. Cormack, Study on distortion conspicuity in stereoscopically viewed 3D images, in: IEEE 10th IVMSP Workshop, 2011, pp. 24–29.
[30] A.B. Watson, J.A. Solomon, Model of visual contrast gain control and pattern masking, Journal of the Optical Society of America 14 (9) (1997) 2379–2391, http://dx.doi.org/10.1364/JOSAA.14.002379.
[31] R. Blake, D.H. Westendorf, R. Overton, What is suppressed during binocular rivalry? Perception 9 (2) (1980) 223–231.
[32] I.T. Kaplan, W. Metlay, Light intensity and binocular rivalry, Journal of Experimental Psychology 67 (1) (1964) 22–26.
[33] P. Whittle, Binocular rivalry and the contrast at contours, Quarterly Journal of Experimental Psychology 17 (3) (1965) 217–226.
[34] W.J.M. Levelt, On Binocular Rivalry, Mouton, The Hague, Paris, 1968.
[35] M. Fahle, Binocular rivalry: suppression depends on orientation and spatial frequency, Vision Research 22 (7) (1982) 787–800.
[36] N.K. Logothetis, J.D. Schall, Neuronal correlates of subjective visual perception, Science (New York, NY) 245 (4919) (1989) 761–763.
[37] D.A. Leopold, N.K. Logothetis, Activity changes in early visual cortex reflect monkeys' percepts during binocular rivalry, Nature 379 (6565) (1996) 549–553.
[38] D. Alais, R. Blake, Grouping visual features during binocular rivalry, Vision Research 39 (26) (1999) 4341–4353.
[39] R. Blake, N.K. Logothetis, Visual competition, Nature Reviews Neuroscience 3 (1) (2002) 13–21.
[40] D.J. Field, A. Hayes, R.F. Hess, Contour integration by the human visual system: evidence for a local "association field", Vision Research 33 (2) (1993) 173–193.
[41] M.K. Kapadia, M. Ito, C.D. Gilbert, G. Westheimer, Improvement in visual sensitivity by changes in local context: parallel studies in human observers and in V1 of alert monkeys, Neuron 15 (4) (1995) 843–856.
[42] B. Julesz, Foundations of Cyclopean Perception, University of Chicago Press, 1971.
[43] A. Klaus, M. Sormann, K. Karner, Segment-based stereo matching using belief propagation and a self-adapting dissimilarity measure, in: Proceedings of the International Conference on Pattern Recognition, vol. 3, 2006, pp. 15–18.
[44] D.J. Field, Relations between the statistics of natural images and the response properties of cortical-cells, Journal of the Optical Society of America 4 (12) (1987) 2379–2394.
[45] C.-C. Su, A.C. Bovik, L.K. Cormack, Natural scene statistics of color and range, in: IEEE International Conference on Image Processing.
[46] C.W. Tyler, Stereoscopic depth movement: two eyes less sensitive than one, Science (New York, NY) 174 (4012) (1971) 958–961.
[47] C. Schor, I. Wood, J. Ogawa, Binocular sensory fusion is limited by spatial resolution, Vision Research 24 (7) (1984) 661–665.
[48] RIEGL, Riegl vz-400 3D Terrestrial Laser Scanner, URL ⟨http://rieglusa.com/products/terrestrial/vz-400/index.shtml⟩.
[49] I.T.U.R. Assembly, U. International Telecommunication, Methodology for the Subjective Assessment of the Quality of Television Pictures, International Telecommunication Union, Geneva, Switzerland, 2003.
[50] Z. Wang, A.C. Bovik, H.R. Sheikh, E.P. Simoncelli, Image quality assessment: from error visibility to structural similarity, IEEE Transactions on Image Processing 13 (4) (2004) 600–612.
[51] H.R. Sheikh, A.C. Bovik, G. de Veciana, An information fidelity criterion for image quality assessment using natural scene statistics, IEEE Transactions on Image Processing 14 (12) (2005) 2117–2128.
[52] F.W. Campbell, D.G. Green, Optical and retinal factors affecting visual resolution, Journal of Physiology 181 (1965) 576–593.
[53] B.N. Vlaskamp, G. Yoon, M.S. Banks, Neural and optical constraints on stereoacuity, in: Perception 37 ECVP Abstract Supplement, 2008, p. 2.
[54] F. Allenmark, J. Read, Spatial stereoresolution, Journal of Vision 9 (8) (2009) 262.
[55] A.K. Moorthy, C. Su, A. Mittal, A.C. Bovik, Subjective evaluation of stereoscopic visual quality, in: Signal Processing: Image Communication, Special Issue on Biologically Inspired Approaches for Visual Information Processing and Analysis, to be published.
[56] M.G. Perkins, Data compression of stereopairs, IEEE Transactions on Communications 40 (4) (1992) 684–696.
[57] A. Vetro, A.M. Tourapis, K. Muller, C. Tao, 3D-TV content storage and transmission, IEEE Transactions on Broadcasting 57 (2) (2011) 384–394.
[58] R. Sekuler, R. Blake, Perception, A.A. Knopf, New York, 1985.
[59] J. Burge, M.A. Peterson, S.E. Palmer, Ordinal configural cues combine with metric disparity in depth perception, Vision 5 (6), Journal of Vision June 22, 2005, http://dx.doi.org/10.1167/5.6.5.
[60] M. Lambooij, W. Ijsselsteijn, D.G. Bouwhuis, I. Heynderickx, Evaluation of stereoscopic images: beyond 2D quality, IEEE Transactions on Broadcasting 57 (2) (2011) 432–444.
[61] M.-J. Chen, D.-K. Kwon, A.C. Bovik, Study of subject agreement on stereoscopic video quality, in: Proceedings of the IEEE Southwest Symposium on Image Analysis and Interpretation.